

# Learning A Low-Level Vision Generalist via Visual Task Prompt

Xiangyu Chen  
University of Macau; Shanghai AI  
Laboratory; Shenzhen Institute of  
Advanced Technology, CAS

Wenlong Zhang  
Shanghai AI Laboratory,  
The Hong Kong Polytechnic  
University

Yihao Liu  
Shanghai AI Laboratory;  
Shenzhen Institute of Advanced  
Technology, CAS

Jiantao Zhou\*  
State Key Laboratory of Internet  
of Things for Smart City,  
University of Macau

Chao Dong\*  
Shanghai AI Laboratory; Shenzhen  
Institute of Advanced Technology,  
CAS; Shenzhen University of  
Advanced Technology

Yuandong Pu  
Shanghai Jiao Tong University,  
Shanghai AI Laboratory

Yu Qiao  
Shanghai AI Laboratory;  
Shenzhen Institute of Advanced  
Technology, CAS

## ABSTRACT

Building a unified model for general low-level vision tasks holds significant research and practical value. Current methods encounter several critical issues. Multi-task restoration approaches can address multiple degradation-to-clean restoration tasks, while their applicability to tasks with different target domains (e.g., image stylization) is limited. Methods like PromptGIP can handle multiple input-target domains but rely on the Masked Autoencoder (MAE) paradigm. Consequently, they are tied to the ViT architecture, resulting in suboptimal image reconstruction quality. In addition, these methods are sensitive to prompt image content and often struggle with low-frequency information processing. In this paper, we propose a Visual task Prompt-based Image Processing (VPIP) framework to overcome these challenges. VPIP employs visual task prompts to manage tasks with different input-target domains and allows flexible selection of backbone network suitable for general tasks. Besides, a new prompt cross-attention is introduced to facilitate interaction between the input and prompt information. Based on the VPIP framework, we train a low-level vision generalist model, namely GenLV, on 30 diverse tasks. Experimental results show that GenLV can successfully address a variety of low-level tasks, significantly outperforming existing methods both quantitatively and qualitatively. Codes are available at <https://github.com/chxy95/GenLV>.

## CCS CONCEPTS

• **Computing methodologies** → **Image representations; Reconstruction; Computational photography.**

\*Corresponding author

Permission to make digital or hard copies of all or part of this work for personal or classroom use is granted without fee provided that copies are not made or distributed for profit or commercial advantage and that copies bear this notice and the full citation on the first page. Copyrights for components of this work owned by others than the author(s) must be honored. Abstracting with credit is permitted. To copy otherwise, or republish, to post on servers or to redistribute to lists, requires prior specific permission and/or a fee. Request permissions from [permissions@acm.org](mailto:permissions@acm.org).

ACM MM, 2024, Melbourne, Australia

© 2024 Copyright held by the owner/author(s). Publication rights licensed to ACM.

ACM ISBN 979-8-4007-0686-8/24/10

<https://doi.org/10.1145/3664647.3681621>

## KEYWORDS

General Low-Level Vision, Image Restoration and Enhancement, Multi-task Learning, Visual Prompt

### ACM Reference Format:

Xiangyu Chen, Yihao Liu, Yuandong Pu, Wenlong Zhang, Jiantao Zhou, Yu Qiao, and Chao Dong. 2024. Learning A Low-Level Vision Generalist via Visual Task Prompt. In *Proceedings of the 32nd ACM International Conference on Multimedia (MM'24)*, October 28–November 1, 2024, Melbourne, Australia. ACM, New York, NY, USA, 13 pages. <https://doi.org/10.1145/3664647.3681621>

## 1 INTRODUCTION

Low-level vision comprises a multitude of tasks that manipulate and enhance the pixel-level information of images. These tasks include but are not limited to image restoration, image enhancement, image feature extraction and image stylization. Over the years, numerous methods have been proposed to address various low-level vision tasks, many of which have achieved commendable performance for specific individual tasks [6, 10, 49]. However, developing task-specific models often proves to be time-consuming and labor-intensive. Recently, there has been a significant trend in artificial intelligence towards creating general models. In Natural Language Processing (NLP), Large Language Models (LLMs) like the GPT series [4, 33] have exhibited remarkable performance. Similarly, in computer vision, models such as the Segment Anything Model (SAM) [24] and Track Anything Model (TAM) [46] have emerged, primarily focusing on high-level perceptual tasks. However, research on general models for low-level tasks is limited.

Designing a general model for low-level vision presents several challenges. Firstly, the diversity of tasks involves distinct input and target domains (e.g., image restoration vs. stylization). Unifying these within a single framework is difficult. Existing models often target specific task categories, such as AirNet [26] and PromptIR [35], which focus on restoration tasks but cannot handle feature extraction or stylization. Secondly, for low-level vision, pixel-level reconstruction quality is crucial. However, existing general vision models focus more on perceptual accuracy, neglecting the model's image reconstruction capability. For instance, MAE-VQGAN [3]

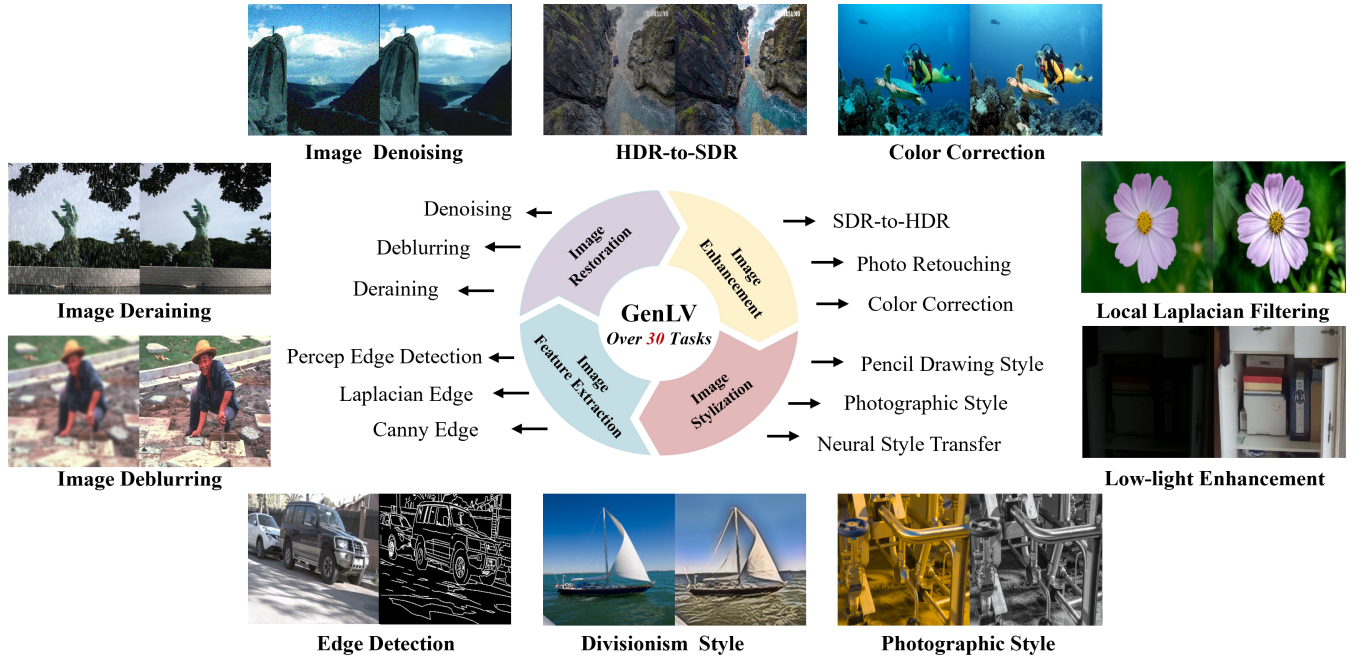


**Figure 1: Our proposed low-level vision generalist model, GenLV, can handle diverse tasks with various input/target domains.**

uses discrete feature representations for image reconstruction, often resulting in unacceptable structural differences between inputs and outputs [30]. Painter [40] and PromptGIP [30], based on ViT architecture [16], often lack fine details and occasionally exhibit blocking artifacts. Furthermore, handling a wider range of low-level tasks involves processing high- and low-frequency information simultaneously, posing additional challenges. PromptGIP [30] performs well within a limited task range, but struggles when tasks increase, especially when more low-frequency information processing (e.g., color and style) is involved. The Painter [40] model trained under the same low-level task settings faces similar or even more severe issues, as shown in Figure 5. These challenges are attributed to the Masked Autoencoder (MAE)-based training paradigm, which makes the models sensitive to the prompt image content, especially for the low-frequency information.

To address these issues, we propose a Visual Task Prompt-based Image Processing (VPIP) framework. It consists of three components: an end-to-end image processing network, a prompt encoder sub-network, and an information interaction mechanism for task-specific processing. We employ the X-Restormer [8] as the main network, which is designed for general image restoration tasks. We take input-target image pairs as visual prompt to represent different tasks. The prompt encoder processes the visual prompt into latent representations, and a new prompt cross-attention is introduced to incorporate the latent task information into the main network.

Our VPIP framework offers several advantages: 1) It effectively solves the problem of varying input-target domains for various tasks. 2) It is not restricted to the MAE paradigm, enhancing robustness against prompt image content. 3) It allows flexibility in selecting backbone networks, improving reconstruction quality. 4) It reduces attention computation costs of global attention in previous MAE-based models by using cross-attention.

To evaluate the effectiveness of our method, we construct 30 diverse tasks to train the model. The trained low-level vision generalist model, namely GenLV, can successfully process the various tasks with different input and target domains, as shown in Figure 1. Comprehensive experiments, detailed in Section 4, demonstrate that GenLV significantly outperforms existing methods.

## 2 RELATED WORK

**Low-Level Vision.** Over the past decade, low-level vision has significantly advanced due to deep learning integration. Classic tasks in this field include image restoration, enhancement, feature extraction, and stylization. Image restoration focuses on recovering high-quality image from degraded versions caused by factors like low-resolution [15], noise [51], blur [1], JPEG compression [14] and bad weather, such as rain [47] and haze [48]. Image enhancement [36] involves modifying image attributes like color [18], sharpness [2], exposure [9] and brightness [7], to improve suitability for specific tasks or viewers. Image feature extraction, extracts low-level features to aid downstream enhancement and understanding tasks. Image stylization aims to create visually appealing images with a specific style or aesthetic [23]. Despite advancements, current methods often depend on specialized datasets and customized network architectures, limiting their practical applications.

**Prompt Learning.** In the NLP field, the concept of prompting is initially to supply manually selected in-context information to a pretrained model for implementing the target task [4]. Instead of using manual prompt, many follow-up works propose to treat the prompt as task-specific vectors to adapt model for various tasks [20, 25]. Prompt learning techniques have also been applied in computer vision, where they have proven effective in modeling task-specific instructions across various applications [21, 52].

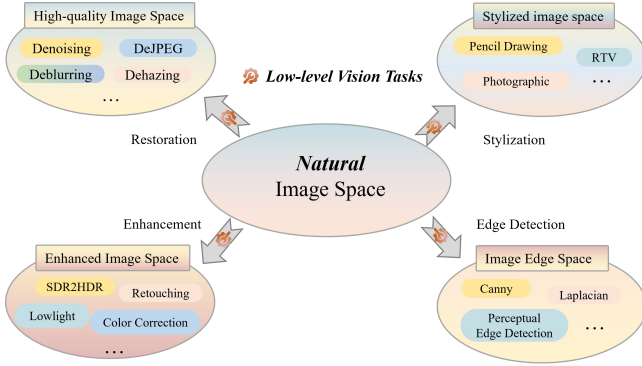


**Figure 2: Diverse low-level vision tasks. Different categories of tasks differ in terms of target domains. It presents a significant challenge to build a low-level vision generalist model.**

Notably, MAE-VQGAN [3] and Painter [40] employ prompting to unify vision tasks, excelling in high-level tasks like semantic segmentation. However, their effectiveness in low-level vision tasks is limited [30]. In the realm of low-level vision, PromptGIP [30] uses an MAE-based framework and grid-like visual prompt for 15 cross-domain tasks. Despite this, as task complexity increases, the effectiveness of this method diminishes. Besides, the training paradigm adopted by PromptGIP highly relies on the ViT architecture, which greatly limits its image reconstruction quality.

**Multi-task Image Restoration.** Multi-task image restoration aims to train a single model to handle multiple restoration tasks simultaneously. Existing multi-task image restoration methods can be categorized into two groups. The first group of methods aim to process real-world images with unknown degradation, emphasizing the modeling of complex real-world degradation. The representative approaches include BSRGAN [50] and Real-ESRGAN [41]. In contrast, the second group of methods like DASR [39] and AirNet [26] are developed to handle several specific restoration tasks with predefined degradation. These methods mainly focus on designing better modules for multi-task learning to maximize network capability of task-specific restoration performance. Some current works such as ProRes [32] and PromptIR [35] are proposed to leverage a learnable prompt from the input image for better multi-task restoration. However, all these approaches are limited to solving the degradation-to-clean restoration problem, and lack the ability to deal with a broad range of cross-domain low-level vision tasks. Unlike these approaches, our method aims to construct a low-level vision generalist model, which is not only capable of image restoration, but also excels at handling a wider range of cross-domain tasks, including enhancement, feature detection and stylization.

### 3 APPROACH

#### 3.1 Representative Low-Level Vision Tasks

Low-level vision tasks encompass a range of pixel-level manipulations, including image restoration, enhancement, feature extraction, stylization, etc. Each task uniquely transforms an input image space to a specific target domain. For example, the target domain of image restoration is high-quality (HQ) image space  $\Omega_{HQ}$ , while the

outputs of edge detection are edges maps  $\Omega_{Edge}$ . Formally, given an arbitrary input image  $I$ , the low-level vision task can be defined as  $\mathcal{T}_{task} : \Omega_S \rightarrow \Omega_T$ , where  $\Omega_S$  and  $\Omega_T$  denote the source image space and the target image space, respectively. According to the target domain, low-level vision tasks generally fall into the following categories as:

$$\begin{aligned} \text{Restoration: } & \mathcal{T}_{Res} : \Omega_S \rightarrow \Omega_{HQ}, \\ \text{Enhancement: } & \mathcal{T}_{Enh} : \Omega_S \rightarrow \Omega_{Enh}, \\ \text{Edge Detection: } & \mathcal{T}_{Edg} : \Omega_S \rightarrow \Omega_{Edg}, \\ \text{Stylization: } & \mathcal{T}_{Sty} : \Omega_S \rightarrow \Omega_{Sty}. \end{aligned} \quad (1)$$

Each category encompasses a variety of tasks, as presented in Figure 2. Our goal is to address all these tasks through a unified model.

#### 3.2 Problem Formulation

Existing low-level vision methods are typically designed for specific tasks, which inherently restricts their applicability to tasks with different target domains. Taking the image restoration model as an example, they accept low-quality images as input and predict the high-quality output as:

$$I_{out} = \mathcal{F}_{\mathcal{T}_{Res}}(I_{in}; \Theta) \in \Omega_{HQ}, \quad (2)$$

where  $\mathcal{F}_{\mathcal{T}_{Res}}$  represents the restoration model parameterized by  $\Theta$ . The restoration model can accommodate various restoration tasks through incorporating multiple degradations into training, such as blur, denoising and deraining, given that the output image space of these tasks are the same, i.e.,  $\Omega_{HQ}$ . However, this kind of model cannot be extended to simultaneously implement tasks like edge detection, which targets a completely different output modality.

To train a low-level vision generalist model that can process cross-domain tasks, our approach employs a unified framework capable of handling various cross-domain tasks by utilizing additional image pair as the prompt  $[P_{\Omega_S}, P_{\Omega_T}]$ . It can be denoted as:

$$I_{out} = \mathcal{F}_{\mathcal{T}}(I_{in}, [P_{\Omega_S}, P_{\Omega_T}]; \Theta). \quad (3)$$

This formulation allows diverse task mappings to be represented by intuitive image pairs, which marks a significant difference from conventional low-level vision models, offering a more holistic and adaptable approach to broad cross-domain low-level vision tasks.

#### 3.3 Low-Level Vision Generalist Model

In this section, we illustrate the specific design of our low-level vision generalist model, as shown in Figure 3. The overall approach is predicated on the Visual task Prompt-based Image Processing (VIP) framework. A powerful image processing network and a prompt encoder network are used to process the input image and the prompt images. A new prompt cross-attention mechanism is introduced to achieve the information interaction among latent representations of the input image and prompt images.

**VIP Framework** consists of an end-to-end image processing main network, a prompt encoder network and a prompt interaction mechanism. Given an input image  $I_{in}$ , it is initially processed to a high-dimensional latent feature  $z_{in}$  through the encoder. In parallel, the paired prompt images  $[P_{\Omega_S}, P_{\Omega_T}]$  are fed into the prompt encoder to generate two high-dimensional representations  $[z_{\Omega_S}^P, z_{\Omega_T}^P]$ , both of which with the same spatial size as  $z_{in}$ . Following this, the

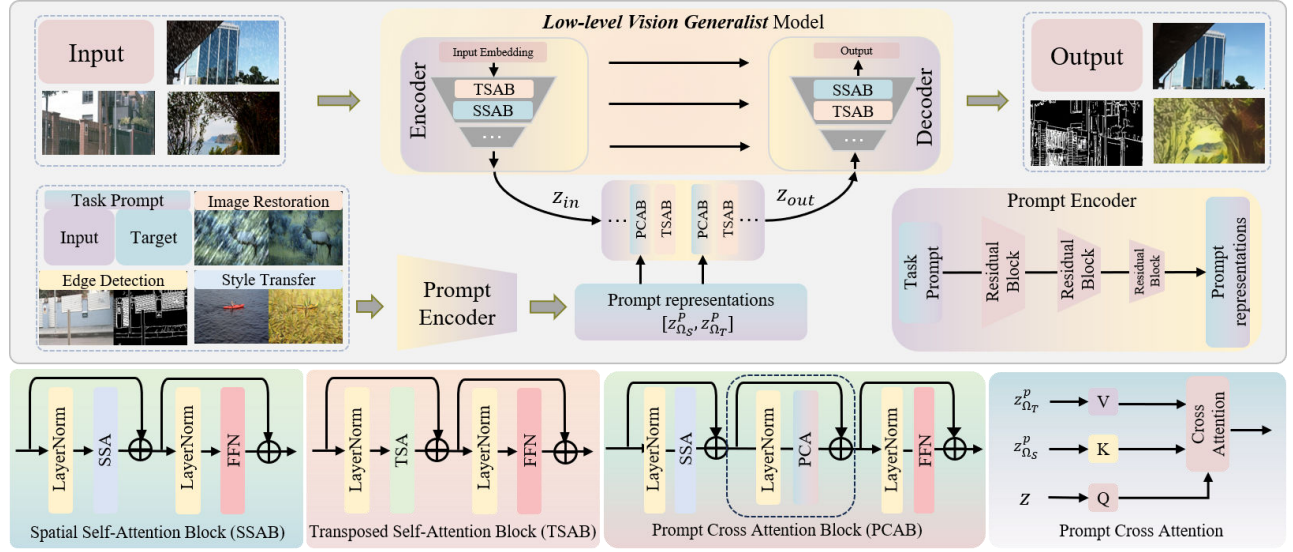


Figure 3: Overall approach of our low-level vision generalist model, GenLV.

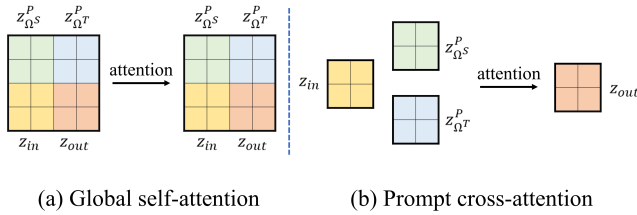


Figure 4: Comparison of two attention mechanisms.

information interaction is implemented between  $z_{in}$  and the pair  $[z_{\Omega_s}^p, z_{\Omega_r}^p]$  and results in the processed latent representation  $z_{out}$ . The final step is to reconstruct the output image from  $z_{out}$  via the decoder in the main network. Unlike previous approaches such as Painter and PromptGIP, which rely on MAE-based framework and require binding with the ViT architecture, our VPIP framework allows flexible selection of backbone networks suitable for low-level vision tasks as the image processing main network.

**Image Processing Backbone** plays a crucial role in the image reconstruction quality for low-level vision tasks. Since different low-level vision tasks often have different requirements for network capability, the most important criterion for selecting a backbone network is its task generality. Due to the lack of work investigating task generality across a wide range of low-level tasks, we focus more on the model performance for image restoration. A recent work conduct a detailed study on the backbone network for restoration tasks and propose a general backbone network, X-Restormer [8], suitable for multiple various restoration tasks. Therefore, we simply adopt similar architecture as our main network<sup>1</sup>. Specifically, the main network employs a U-shape architecture, where down-sampling and up-sampling operations are performed three times,

<sup>1</sup>We also conduct an extensive study on the model performance of different backbone network, and the detailed results are presented in the Supplementary Material.

and skip connections are added from the encoder to the decoder at the same scale. The basic modules to construct the network are Transposed Self-Attention Block (TSAB) and Spatial Self-Attention Block (SSAB), which deal with the channel-wise global information interaction and the spatial information interaction, respectively. The structures of TSAB and SSAB are shown in Figure 3. The implementation details of their attention mechanism can be referred to the OCA in HAT [11] and the MDTA in Restormer [49].

**Prompt Cross-attention** is designed to perform information interaction among the prompt and input representations. PromptGIP [30] demonstrates that calculating global attention in the feature space can effectively incorporate task prompt information into image processing. However, this approach is tightly coupled with the ViT architecture and is relatively inefficient in terms of the attention computation. Inspired by the Stable Diffusion [38] model, which utilizes cross-attention to apply text prompt to the denoising UNet, we adopt a similar mechanism to introduce visual prompt information into the image processing network. As depicted in Figure 3, the Prompt Cross-Attention Block (PCAB) is implemented by adding a PCA module to the standard SSAB and is integrated at the bottom of the U architecture. To calculate the PCA, the *query* ( $Q$ ), *key* ( $K$ ) and *value* ( $V$ ) are first generated by  $1 \times 1$  convolutions from the input representation  $z_{in}$ , prompt input embedding  $z_{\Omega_s}^p$  and prompt target embedding  $z_{\Omega_r}^p$ . Then, the standard attention is computed to obtain the output representation  $z_{out}$ . Compared to calculating global self-attention on the grid-like features consisting of four image representations across the entire network, our prompt cross-attention calculated based on the size of one image representation in just a few blocks (i.e., PCAB) is much more efficient in terms of attention computation, as shown in Figure 4.

**Prompt Encoder** is employed to encode the prompt images into deep representations that can be used for information interaction. We simply utilize a series of standard residual blocks spaced by multiple downsampling operations to build the encoder network.

## 4 EXPERIMENTS AND ANALYSIS

### 4.1 Experimental Setup

**Task Settings.** We train the models on **30** diverse low-level tasks, as follows: 1) **Image Restoration:** Following PromptGIP [30], ten classic degradation types are considered including Gaussian noise, Gaussian blur, Poisson noise, salt & pepper noise, JPEG compression, ringing artifacts, R-L algorithm [37], inpainting, haze and rain. During the training, the on-the-fly data pairs are generated on ImageNet [13] for the first eight types. Simple mixed degradations are also considered for training. ITS dataset [27] and Rain13K [22] are utilized for dehazing and deraining. A simple additive rain model is also employed for synthetic data. For testing, a mixed dataset, Common528 [30], composed of several low-level vision benchmark datasets is employed. 2) **Image Enhancement:** This category includes eight tasks: low-light enhancement (LLE), photo retouching, local Laplacian filtering [2] (LLF), multi-scale tone manipulation (MTM) [17], underwater image contrast enhancement (ICE) based on histogram equalization, underwater image color correction (ICC) based on the DIVE+ software, image SDR-to-HDR and HDR-to-SDR [12]. The LOL dataset [43] is used for LLE, and expert-C retouched images of the Adobe-MIT Fivek dataset [5] are used for retouching, LLF, and MTM. The UIEB dataset [28] is utilized for the two underwater image enhancement tasks. 3) **Image Edge Detection:** This category includes three edge detection tasks: Canny operator, Laplacian operator and a perceptual edge detection (PED) [34]. 4) **Image Stylization:** Nine style are chosen, including pencil drawing [31], photographic style [2], relative total variation (RTV) [45], Vermeer style, JOJO style, Raphael style, Fauvism style, Divisionism style and Cloisonnism style. Expert-C retouched images of Adobe-MIT Fivek dataset [5] are also used to generate the image pairs. Data of the first three styles are implemented via available toolkit, and the last six neural styles are generated by a state-of-the-art style transfer method AdaAttN [29].

**Implement details.** For the backbone network, we adopt the similar setting as the original X-Restormer [8]. From level-1 to level-4, the numbers of consecutive blocks (each block contains a TSAB and an SSAB) are [2, 4, 4, 4], attention heads in TSA and SSA are both [1, 2, 4, 8], and channel numbers are [48, 96, 192, 384]. For the prompt encoder network, we employ four residual blocks for each downsampling level. During the training, the input size is set to  $256 \times 256$  for the input image and prompt images.  $L_1$  loss is utilized as the loss function. AdamW optimizer with  $\beta_1 = 0.9$  and  $\beta_2 = 0.99$  is adopted with an initial learning rate of  $1e^{-4}$ . The batch size is set to 64 and total training epochs are 30.

### 4.2 Quantitative Results

The quantitative results for various low-level vision tasks are presented in Table 1, Table 2 and Table 3. Given that not all existing methods are capable to handle tasks across different target domains, our primary comparative experiments are centered on restoration tasks in Table 1. We consider three distinct experimental settings. The first setting utilizes a pretrained model, i.e., Real-ESRGAN [41], which is capable of handling a variety of restoration tasks. The second setting is based on the training configuration outlined in our paper, but it solely focuses on image restoration tasks. The third setting involves training on the all 30 low-level vision tasks.

**Ablation Study on Visual Prompt.** Since the models without using task prompt cannot process tasks with different target domains, we conduct the ablation study of the visual task prompt on restoration tasks. In Table 1, ViT\* and X-Restormer\* are two end-to-end models only trained on image restoration tasks, while ViT-VPIP\* and GenLV\* (the GenLV model can also be represented as X-Restormer-VPIP) are models based on our VPIP framework, utilizing ViT and X-Restormer as their backbone respectively. Upon the incorporation of prompt learning, both ViT-VPIP\* and GenLV\* exhibit substantial performance gains over ViT\* and X-Restormer\* in most restoration tasks. This demonstrates the effectiveness of the visual prompt in facilitating the backbone network to better handle various tasks. It is noteworthy that X-Restormer\*, without using visual prompt, struggles with the dehazing task, achieving only 16.73dB. A similar phenomenon also occurs for the multi-task restoration method PromptIR [35]. In contrast, GenLV\* tackles it considerably better, reaching 25.63dB. All these results show the effectiveness of our proposed VPIP framework.

**Influence of Backbone Network.** In Table 1, when trained on the same setting, the performance of models using X-Restormer as the backbone network (i.e., X-Restormer\*, GenLV\* and GenLV<sup>†</sup>) significantly surpasses that of models using ViT (i.e., ViT\*, ViT-VPIP\* and ViT-VPIP<sup>†</sup>). This observation suggests that an appropriate backbone network is important for low-level vision tasks generalist models, and ViT architecture may limit the model performance.

**Comparison with other methods.** In Table 1, GenLV\* outperforms the state-of-the-art blind SR method Real-ESRGAN [41] and multi-task restoration method PromptIR [35], when only considering image restoration tasks. Note that we retrain the PromptIR model on the same setting for fair comparison (the original PromptIR is trained only on 4 tasks). By employing the ViT network, PromptGIP\* trained on restoration tasks performs better than ViT-VPIP\*, due to more attention computation. However, as more tasks are involved, ViT-VPIP<sup>†</sup> outperforms PromptGIP<sup>†</sup> and Painter<sup>†</sup> instead, showing the superiority of our framework for solving more diverse tasks. In Table 2 and Table 3, we further show the quantitative results on broader low-level vision tasks. Only methods capable of solving tasks across different target domains are considered in the comparison. The models employed VPIP framework outperform Painter and PromptGIP on a variety of low-level vision tasks.

### 4.3 Visual Results

In Figure 5, we present the visual comparison of our GenLV with Painter and PromptGIP across various low-level vision tasks. From a holistic perspective, GenLV produces results that are more consistent with the ground truth, especially in aspects such as color and brightness. In contrast, the results produced by Painter and PromptGIP are easily affected by errors in low-frequency information, manifesting as color anomalies or even incorrect task execution. Rather than our method where prompt information can accurately serve as task instruction, Painter and PromptGIP appear to be significantly affected by the content of the prompt image. In terms of image reconstruction quality, the images generated by GenLV have clear textures and details. Conversely, Painter and PromptGIP may suffer from blurring or blocking artifacts, particularly for image restoration tasks. Overall, the above results show the superiority of GenLV in visual quality for dealing with various low-level tasks.

**Table 1: Quantitative results on image restoration tasks. #: public released model. ★: trained with only restoration tasks. †: trained with all 30 low-level vision tasks. GN: Gaussian noise. PN: Poisson noise. ViT-VPIP: ViT backbone adopted in the VPIP framework. Our GenLV can also be represented as X-Restormer-VPIP. PSNR↑ (dB) is calculated as the quantitative metric.**

	GN	PN	S&P Noise	GB	JPEG	Ringling	R-L	Inpainting	SimpleRain	ComplexRain	Haze
Real-ESRGAN#	25.38	26.57	21.50	21.49	25.21	24.64	21.71	14.06	16.10	21.01	11.86
PromptIR★	28.86	31.48	36.45	24.56	26.77	<b>27.85</b>	31.31	<b>28.11</b>	30.76	24.08	16.85
PromptGIP★	26.48	27.76	28.08	22.88	25.86	25.69	27.05	25.28	25.79	24.33	24.55
ViT★	24.67	25.39	23.71	22.17	24.76	23.89	24.09	23.11	23.21	23.04	24.91
ViT-VPIP★	26.14	27.20	25.43	24.13	26.19	25.98	26.98	25.03	25.51	<b>24.79</b>	24.06
X-Restormer★	28.70	31.36	35.33	24.13	26.68	26.88	30.01	27.68	29.65	24.39	16.73
GenLV★ (ours)	<b>28.99</b>	<b>31.69</b>	<b>36.63</b>	<b>24.58</b>	<b>26.91</b>	27.74	<b>31.50</b>	<b>28.11</b>	<b>31.10</b>	24.71	<b>28.91</b>
Painter†	24.28	24.41	24.93	21.55	22.30	23.58	24.36	22.52	22.42	23.14	20.20
PromptGIP†	23.63	23.98	25.05	20.84	22.21	23.86	24.94	22.11	23.16	21.79	21.90
ViT-VPIP†	25.30	26.15	24.41	22.74	25.35	24.62	25.24	23.73	24.00	23.70	24.04
GenLV† (ours)	<b>28.49</b>	<b>31.05</b>	<b>34.20</b>	<b>23.39</b>	<b>26.21</b>	<b>25.78</b>	<b>28.21</b>	<b>27.17</b>	<b>28.18</b>	<b>25.11</b>	<b>29.70</b>

**Table 2: Quantitative results on image enhancement and stylization tasks. PSNR↑ (dB) is calculated as the quantitative metric.**

	LowLight	LLF	Retouching	ICC	ICE	MTM	SDR2HDR	HDR2SDR	PencilDraw	Photographic	RTV
Painter†	20.19	23.98	18.29	21.62	15.89	21.51	25.63	20.56	16.79	22.68	26.69
PromptGIP†	18.60	25.40	20.44	24.29	16.16	20.84	26.40	18.87	17.74	21.68	30.29
ViT-VPIP†	22.16	23.78	22.01	27.70	16.86	26.10	27.89	23.91	19.56	22.30	31.89
GenLV† (ours)	<b>23.55</b>	<b>27.61</b>	<b>23.84</b>	<b>35.44</b>	<b>17.36</b>	<b>31.59</b>	<b>34.45</b>	<b>35.92</b>	<b>20.00</b>	<b>23.86</b>	<b>33.03</b>

**Table 3: Quantitative results on edge detection tasks. Mean absolute error↓ is calculated as the quantitative metric.**

	Canny	Laplacian	PED
Painter†	31.36	7.06	9.55
PromptGIP†	19.48	4.06	9.36
ViT-VPIP†	27.68	5.49	8.44
GenLV† (ours)	<b>8.07</b>	<b>1.27</b>	<b>7.23</b>

**Table 4: Standard deviation of the performance computed based on 20 different prompt images. PSNR (dB) is calculated as the quantitative metrics.**

	GN	GB	LowLight	ICC	PencilDraw	RTV
Painter†	2.3930	1.8845	1.8865	1.9573	1.1820	2.6163
PromptGIP†	3.1035	2.2893	0.6766	0.6311	1.4200	1.3130
GenLV†	<b>0.1033</b>	<b>0.0208</b>	<b>0.0399</b>	<b>0.0512</b>	<b>0.5518</b>	<b>0.0195</b>

#### 4.4 Exploration of Task Prompt

The above results have demonstrated the advantages of our prompt mechanism compared to existing methods from quantitative and qualitative perspectives. In this section, we conduct more experiments to further illustrate the effectiveness and explore the limitation of the task prompt in our method.

**Influence of Different Prompts.** To explore the influence on the quantitative performance for different prompt images, we randomly select 20 prompt image pairs for each task and calculate the performance on the corresponding test sets. Then, we compute the standard deviation of the 20 performance results for each task, as shown in Table 4. We can see that except for PencilDraw, the standard deviations are around or lower than 0.1dB. This shows that our method is stable in performance for different prompts.

**Task Prompt on Complex Situations.** We conduct further experiments to investigate the effectiveness of task prompt on complex situations. In Figure 6(a), we exhibit the outputs for images subjected to mixed degradation. The results show that the task prompt

successfully guide the mapping under this situation, and our method has the capability to deal with tasks with mixed degradation. In Figure 6(b), we present the results for cross-domain prompt. Utilizing Canny edge detection and LLE prompts, we instruct the model to process the noisy images. We can see that our model accurately execute the target task according to the visual prompts other than perform denoising. In Figure 6(c), we show the results on processing mixed degraded images using single-task prompts. The first row present the application of a denoising prompt to a low-light, noisy image. In the second row, we show that a deraining prompt is applied to a blurry image rain streaks. It can be see that the task-specific prompts effectively guide the model to perform the target task. All these results demonstrate the effectiveness of the visual task prompt in our method across a variety of complex situations.

**Mismatch Test.** We conduct mismatch test to illustrate the impact of the prompt on the model under special scenarios, as shown in Figure 7. The first row demonstrates providing the deblurring prompt to a clean image. In the second and third rows, we provide

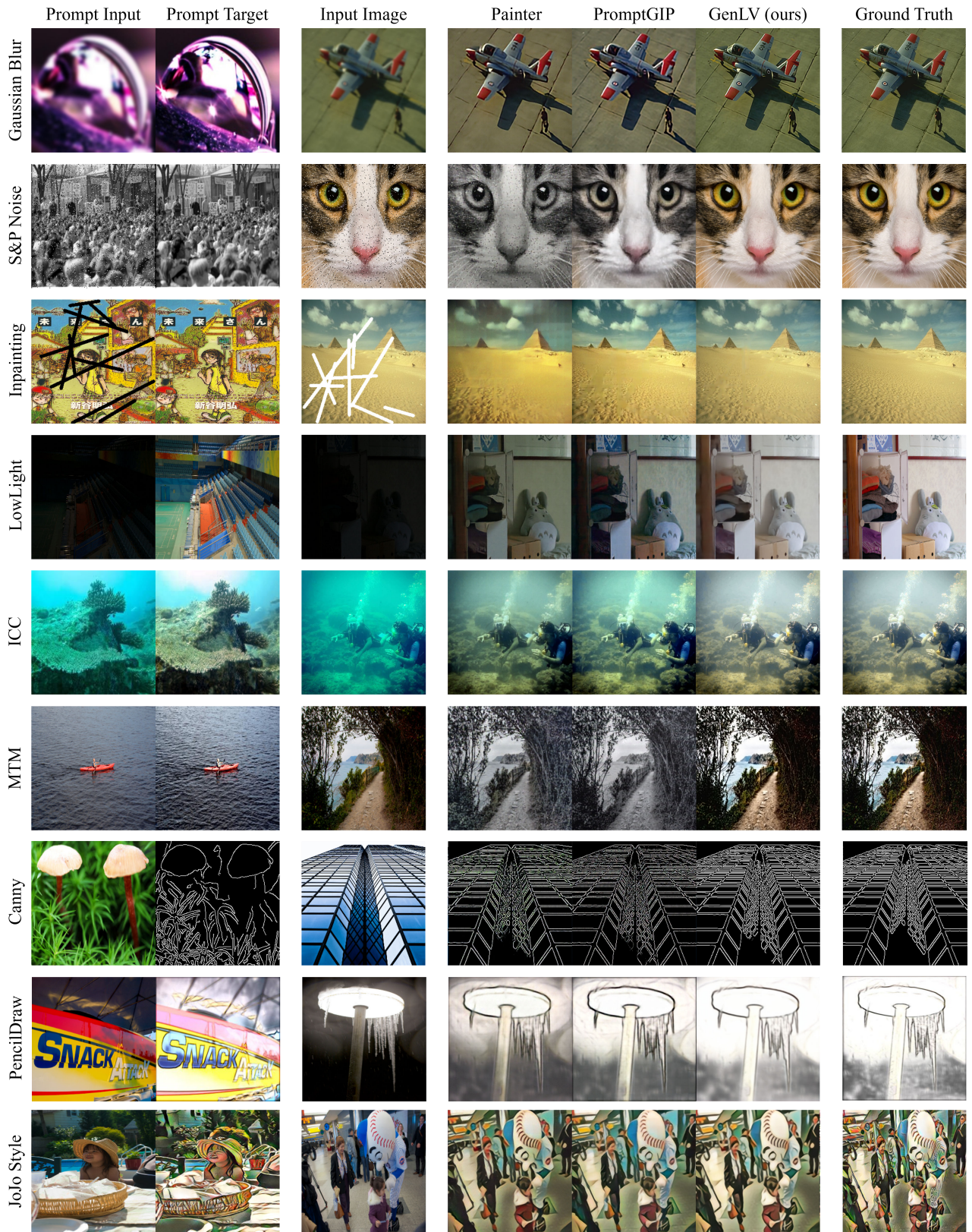
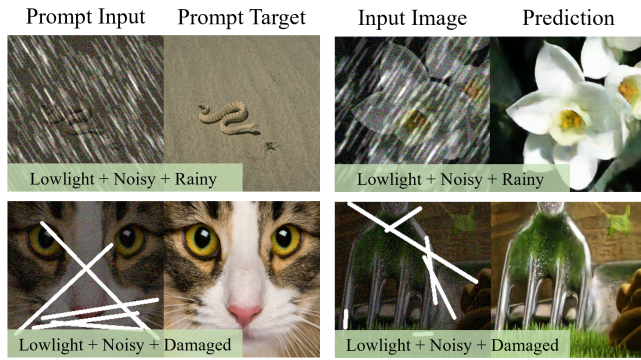
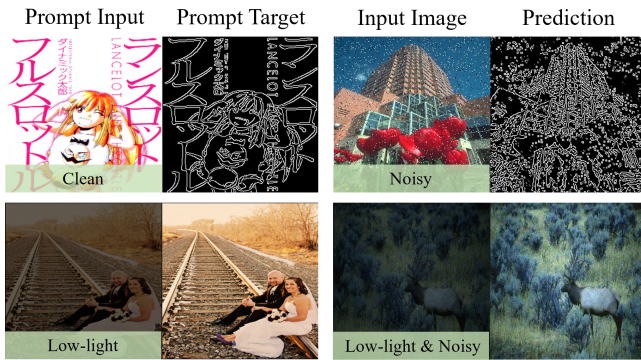


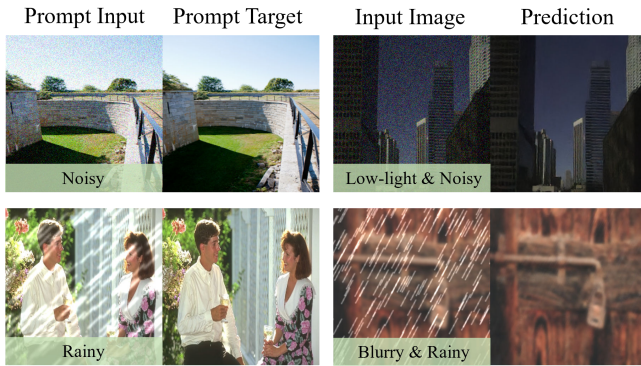
Figure 5: Visual results of different models on various low-level vision tasks.



(a) Results for mixed degraded images.



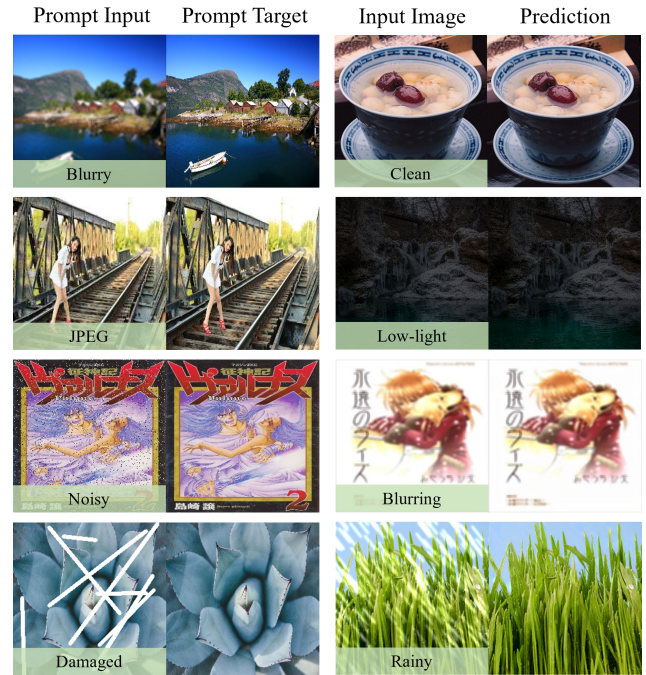
(b) Results for images based on cross-domain prompts.



(c) Results for mixed degraded images on single-task prompts.

**Figure 6: Results for task prompts on complex situations.**

deJPEG and denoising prompts for low-light and blurry images, respectively. Ideally, we hope that the model do not execute the wrong prompt (this is reasonable from the perspective of the prompt cross-attention mechanism). It is observed that the model ideally preserves the original input images instead of performing degradation removal in these three instances. However, the mismatch test does not consistently yield ideal outcomes. In the fourth row, the model conducts deraining when provided with an inpainting prompt. From this perspective, this indicates that the model still inevitably overfit some data or mappings during training.

**Figure 7: Results of the mismatch test.**

## 5 LIMITATIONS AND PROSPECTS

Our GenLV model demonstrates commendable performance in solving a broad range of low-level vision tasks, leveraging the visual prompt-based image processing framework and a powerful backbone network. Nonetheless, there are certain limitations and potential areas for further exploration that warrant attention. The working mechanism of this method is still to divide the task space via visual prompt, to achieve multi-task low-level vision. Despite the considerable improvement in performance compared to existing methods, we have to claim that the model currently still lacks the ability to generate satisfactory results for out-of-distribution unseen tasks. Recent study about large language models (LLMs) underscore that the effectiveness of LLMs largely depends on the quality, diversity, and quantity of the training data [44]. However, the task variety, model size (~30M), data scale (~140W) are not sufficient for GenLV. We hope that future studies involving larger models, broader tasks and data will yield more surprising results.

## 6 CONCLUSION

In this paper, we introduce a low-level vision generalist model, GenLV, which is capable of addressing various low-level vision tasks. Our approach involves the design of an image processing framework based on visual task prompt, VPIP, which enables the model to accommodate multiple tasks with different target domains. In addition, this framework allows the flexibility to incorporate a powerful backbone network that is suitable for low-level vision tasks, resulting in superior image reconstruction quality. Experimental results demonstrate that our GenLV can effectively manage 30 diverse low-level vision tasks and significantly outperform existing methods quantitatively and qualitatively.



## ACKNOWLEDGMENTS

This work was partially supported by National Natural Science Foundation of China (Grant No.62276251, 62272450), and the Joint Lab of CAS-HK. This work was also supported in part by Macau Science and Technology Development Fund under SKLIOTSC-2021-2023 and 0022/2022/A.

## REFERENCES

- [1] Abdullah Abuolaim and Michael S Brown. 2020. Defocus deblurring using dual-pixel data. In *Computer Vision—ECCV 2020: 16th European Conference, Glasgow, UK, August 23–28, 2020, Proceedings, Part X 16*. Springer, 111–126.
- [2] Mathieu Aubry, Sylvain Paris, Samuel W Hasinoff, Jan Kautz, and Frédo Durand. 2014. Fast local laplacian filters: Theory and applications. *ACM Transactions on Graphics (TOG)* 33, 5 (2014), 1–14.
- [3] Amir Bar, Yossi Gandelsman, Trevor Darrell, Amir Globerson, and Alexei Efros. 2022. Visual prompting via image inpainting. *Advances in Neural Information Processing Systems* 35 (2022), 25005–25017.
- [4] Tom Brown, Benjamin Mann, Nick Ryder, Melanie Subbiah, Jared D Kaplan, Prafulla Dhariwal, Arvind Neelakantan, Pranav Shyam, Girish Sastry, Amanda Askell, et al. 2020. Language models are few-shot learners. *Advances in neural information processing systems* 33 (2020), 1877–1901.
- [5] Vladimir Bychkovsky, Sylvain Paris, Eric Chan, and Frédo Durand. 2011. Learning photographic global tonal adjustment with a database of input/output image pairs. In *CVPR 2011*. IEEE, 97–104.
- [6] Yuanhao Cai, Hao Bian, Jing Lin, Haoqian Wang, Radu Timofte, and Yulun Zhang. 2023. Retinexformer: One-stage Retinex-based Transformer for Low-light Image Enhancement. *arXiv preprint arXiv:2303.06705* (2023).
- [7] Chen Chen, Qifeng Chen, Jia Xu, and Vladlen Koltun. 2018. Learning to see in the dark. In *Proceedings of the IEEE conference on computer vision and pattern recognition*. 3291–3300.
- [8] Xiangyu Chen, Zheyuan Li, Yuandong Pu, Yihao Liu, Jiantao Zhou, Yu Qiao, and Chao Dong. 2023. A Comparative Study of Image Restoration Networks for General Backbone Network Design. *arXiv preprint arXiv:2310.11881* (2023).
- [9] Xiangyu Chen, Yihao Liu, Zhengwen Zhang, Yu Qiao, and Chao Dong. 2021. HDRUNet: Single Image HDR Reconstruction With Denoising and Dequantization. In *Proceedings of the IEEE/CVF Conference on Computer Vision and Pattern Recognition (CVPR) Workshops*. 354–363.
- [10] Xiangyu Chen, Xintao Wang, Wenlong Zhang, Xiangtao Kong, Yu Qiao, Jiantao Zhou, and Chao Dong. 2023. HAT: Hybrid Attention Transformer for Image Restoration. *arXiv preprint arXiv:2309.05239* (2023).
- [11] Xiangyu Chen, Xintao Wang, Jiantao Zhou, Yu Qiao, and Chao Dong. 2023. Activating more pixels in image super-resolution transformer. In *Proceedings of the IEEE/CVF Conference on Computer Vision and Pattern Recognition*. 22367–22377.
- [12] Xiangyu Chen, Zhengwen Zhang, Jimmy S Ren, Lynhoo Tian, Yu Qiao, and Chao Dong. 2021. A new journey from SDRTV to HDRTV. In *Proceedings of the IEEE/CVF International Conference on Computer Vision*. 4500–4509.
- [13] Jia Deng, Wei Dong, Richard Socher, Li-Jia Li, Kai Li, and Li Fei-Fei. 2009. Imagenet: A large-scale hierarchical image database. In *2009 IEEE conference on computer vision and pattern recognition*. Ieee, 248–255.
- [14] Chao Dong, Yubin Deng, Chen Change Loy, and Xiaoou Tang. 2015. Compression artifacts reduction by a deep convolutional network. In *Proceedings of the IEEE international conference on computer vision*. 576–584.
- [15] Chao Dong, Chen Change Loy, Kaiming He, and Xiaoou Tang. 2014. Learning a deep convolutional network for image super-resolution. In *European conference on computer vision*. Springer, 184–199.
- [16] Alexey Dosovitskiy, Lucas Beyer, Alexander Kolesnikov, Dirk Weissenborn, Xiuhua Zhai, Thomas Unterthiner, Mostafa Dehghani, Matthias Minderer, Georg Heigold, Sylvain Gelly, Jakob Uszkoreit, and Neil Houlsby. 2021. An Image is Worth 16x16 Words: Transformers for Image Recognition at Scale. In *International Conference on Learning Representations*. <https://openreview.net/forum?id=YicbFdNTTy>
- [17] Zeev Farbman, Raanan Fattal, Dani Lischinski, and Richard Szeliski. 2008. Edge-preserving decompositions for multi-scale tone and detail manipulation. *ACM transactions on graphics (TOG)* 27, 3 (2008), 1–10.
- [18] Michaël Gharbi, Jiawen Chen, Jonathan T Barron, Samuel W Hasinoff, and Frédo Durand. 2017. Deep bilateral learning for real-time image enhancement. *ACM Transactions on Graphics (TOG)* 36, 4 (2017), 1–12.
- [19] Jingwen He, Yihao Liu, Yu Qiao, and Chao Dong. 2020. Conditional sequential modulation for efficient global image retouching. In *Computer Vision—ECCV 2020: 16th European Conference, Glasgow, UK, August 23–28, 2020, Proceedings, Part XIII 16*. Springer, 679–695.
- [20] Edward J Hu, Yelong Shen, Phillip Wallis, Zeyuan Allen-Zhu, Yuanzhi Li, Shean Wang, Lu Wang, and Weizhu Chen. 2021. Lora: Low-rank adaptation of large language models. *arXiv preprint arXiv:2106.09685* (2021).
- [21] Menglin Jia, Luming Tang, Bor-Chun Chen, Claire Cardie, Serge Belongie, Bharath Hariharan, and Ser-Nam Lim. 2022. Visual prompt tuning. In *European Conference on Computer Vision*. Springer, 709–727.
- [22] Kui Jiang, Zhongyuan Wang, Peng Yi, Chen Chen, Baojin Huang, Yimin Luo, Jiayi Ma, and Junjun Jiang. 2020. Multi-scale progressive fusion network for single image deraining. In *Proceedings of the IEEE/CVF conference on computer vision and pattern recognition*. 8346–8355.
- [23] Justin Johnson, Alexandre Alahi, and Li Fei-Fei. 2016. Perceptual losses for real-time style transfer and super-resolution. In *Computer Vision—ECCV 2016: 14th European Conference, Amsterdam, The Netherlands, October 11–14, 2016, Proceedings, Part II 14*. Springer, 694–711.
- [24] Alexander Kirillov, Eric Mintun, Nikhila Ravi, Hanzi Mao, Chloe Rolland, Laura Gustafson, Tete Xiao, Spencer Whitehead, Alexander C. Berg, Wan-Yen Lo, Piotr Dollár, and Ross Girshick. 2023. Segment Anything. *arXiv:2304.02643* (2023).
- [25] Brian Lester, Rami Al-Rfou, and Noah Constant. 2021. The power of scale for parameter-efficient prompt tuning. *arXiv preprint arXiv:2104.08691* (2021).
- [26] Boyun Li, Xiao Liu, Peng Hu, Zhongqin Wu, Jiancheng Lv, and Xi Peng. 2022. All-in-one image restoration for unknown corruption. In *Proceedings of the IEEE/CVF Conference on Computer Vision and Pattern Recognition*. 17452–17462.
- [27] Boyi Li, Wenqi Ren, Dengpan Fu, Dacheng Tao, Dan Feng, Wenjun Zeng, and Zhangyang Wang. 2018. Benchmarking single-image dehazing and beyond. *IEEE Transactions on Image Processing* 28, 1 (2018), 492–505.
- [28] Chongyi Li, Chunle Guo, Wenqi Ren, Runmin Cong, Junhui Hou, Sam Kwong, and Dacheng Tao. 2019. An underwater image enhancement benchmark dataset and beyond. *IEEE Transactions on Image Processing* 29 (2019), 4376–4389.
- [29] Songhua Liu, Tianwei Lin, Dongliang He, Fu Li, Meiling Wang, Xin Li, Zhengxing Sun, Qian Li, and Errui Ding. 2021. Adaattn: Revisit attention mechanism in arbitrary neural style transfer. In *Proceedings of the IEEE/CVF international conference on computer vision*. 6649–6658.
- [30] Yihao Liu, Xiangyu Chen, Xianzheng Ma, Xintao Wang, Jiantao Zhou, Yu Qiao, and Chao Dong. 2023. Unifying image processing as visual prompting question answering. *arXiv preprint arXiv:2310.10513* (2023).
- [31] Cewu Lu, Li Xu, and Jiaya Jia. 2012. Combining sketch and tone for pencil drawing production. In *Proceedings of the symposium on non-photorealistic animation and rendering*. 65–73.
- [32] Jiaqi Ma, Tianheng Cheng, Guoli Wang, Qian Zhang, Xinggang Wang, and Lefei Zhang. 2023. ProRes: Exploring Degradation-aware Visual Prompt for Universal Image Restoration. *arXiv preprint arXiv:2306.13653* (2023).
- [33] Long Ouyang, Jeffrey Wu, Xu Jiang, Diogo Almeida, Carroll Wainwright, Pamela Mishkin, Chong Zhang, Sandhini Agarwal, Katarina Slama, Alex Ray, et al. 2022. Training language models to follow instructions with human feedback. *Advances in Neural Information Processing Systems* 35 (2022), 27730–27744.
- [34] Xavier Soria Poma, Edgar Riba, and Angel Sappa. 2020. Dense extreme inception network: Towards a robust cnn model for edge detection. In *Proceedings of the IEEE/CVF winter conference on applications of computer vision*. 1923–1932.
- [35] Vaishnav Potlapalli, Syed Waqas Zamir, Salman Khan, and Fahad Shahbaz Khan. 2023. PromptIR: Prompting for All-in-One Blind Image Restoration. *arXiv preprint arXiv:2306.13090* (2023).
- [36] Yunliang Qi, Zhen Yang, Wenhao Sun, Meng Lou, Jing Lian, Wenwei Zhao, Xiangyu Deng, and Yide Ma. 2021. A comprehensive overview of image enhancement techniques. *Archives of Computational Methods in Engineering* (2021), 1–25.
- [37] William Hadley Richardson. 1972. Bayesian-based iterative method of image restoration. *JoSA* 62, 1 (1972), 55–59.
- [38] Robin Rombach, Andreas Blattmann, Dominik Lorenz, Patrick Esser, and Björn Ommer. 2022. High-resolution image synthesis with latent diffusion models. In *Proceedings of the IEEE/CVF conference on computer vision and pattern recognition*. 10684–10695.
- [39] Longguang Wang, Yingqian Wang, Xiaoyu Dong, Qingyu Xu, Jungang Yang, Wei An, and Yulan Guo. 2021. Unsupervised degradation representation learning for blind super-resolution. In *Proceedings of the IEEE/CVF Conference on Computer Vision and Pattern Recognition*. 10581–10590.
- [40] Xinlong Wang, Wen Wang, Yue Cao, Chunhua Shen, and Tiejun Huang. 2023. Images speak in images: A generalist painter for in-context visual learning. In *Proceedings of the IEEE/CVF Conference on Computer Vision and Pattern Recognition*. 6830–6839.
- [41] Xintao Wang, Liangbin Xie, Chao Dong, and Ying Shan. 2021. Real-esrgan: Training real-world blind super-resolution with pure synthetic data. In *Proceedings of the IEEE/CVF international conference on computer vision*. 1905–1914.
- [42] Xintao Wang, Ke Yu, Chao Dong, and Chen Change Loy. 2018. Recovering realistic texture in image super-resolution by deep spatial feature transform. In *Proceedings of the IEEE conference on computer vision and pattern recognition*. 606–615.
- [43] Chen Wei, Wenjing Wang, Wenhan Yang, and Jiaying Liu. 2018. Deep retinex decomposition for low-light enhancement. *arXiv preprint arXiv:1808.04560* (2018).
- [44] Jerry Wei, Jason Wei, Yi Tay, Dustin Tran, Albert Webson, Yifeng Lu, Xinyun Chen, Hanxiao Liu, Da Huang, Denny Zhou, et al. 2023. Larger language models

- do in-context learning differently. *arXiv preprint arXiv:2303.03846* (2023).
- [45] Li Xu, Qiong Yan, Yang Xia, and Jiaya Jia. 2012. Structure extraction from texture via relative total variation. *ACM transactions on graphics (TOG)* 31, 6 (2012), 1–10.
- [46] Jinyu Yang, Mingqi Gao, Zhe Li, Shang Gao, Fangjing Wang, and Feng Zheng. 2023. Track anything: Segment anything meets videos. *arXiv preprint arXiv:2304.11968* (2023).
- [47] Wenhan Yang, Robby T Tan, Jiashi Feng, Jiaying Liu, Zongming Guo, and Shuicheng Yan. 2017. Deep joint rain detection and removal from a single image. In *Proceedings of the IEEE conference on computer vision and pattern recognition*. 1357–1366.
- [48] Wenhan Yang, Robby T Tan, Jiashi Feng, Jiaying Liu, Zongming Guo, and Shuicheng Yan. 2017. Deep joint rain detection and removal from a single image. In *Proceedings of the IEEE conference on computer vision and pattern recognition*. 1357–1366.
- [49] Syed Waqas Zamir, Aditya Arora, Salman Khan, Munawar Hayat, Fahad Shahbaz Khan, and Ming-Hsuan Yang. 2022. Restormer: Efficient transformer for high-resolution image restoration. In *Proceedings of the IEEE/CVF Conference on Computer Vision and Pattern Recognition*. 5728–5739.
- [50] Kai Zhang, Jingyun Liang, Luc Van Gool, and Radu Timofte. 2021. Designing a practical degradation model for deep blind image super-resolution. In *Proceedings of the IEEE/CVF International Conference on Computer Vision*. 4791–4800.
- [51] Kai Zhang, Wangmeng Zuo, Yunjin Chen, Deyu Meng, and Lei Zhang. 2017. Beyond a gaussian denoiser: Residual learning of deep cnn for image denoising. *IEEE transactions on image processing* 26, 7 (2017), 3142–3155.
- [52] Kaiyang Zhou, Jingkang Yang, Chen Change Loy, and Ziwei Liu. 2022. Learning to prompt for vision-language models. *International Journal of Computer Vision* 130, 9 (2022), 2337–2348.

## A EXPLORATION ON DIFFERENT IMAGE RESTORATION BACKBONE NETWORKS

The quantitative comparison of various backbone networks for different image restoration tasks is presented in Table 6. All the models are trained on the same multi-task restoration setting. We explore the different backbone networks based on image restoration because it has a clear quantitative evaluation scheme (i.e., PSNR/SSIM) and numerous low-level vision networks are designed based on it. As one can see that the overall performance of X-Restormer is the best, so it is selected as the backbone network in our method. It is noteworthy that the dehazing results show unusual performance, as both Restormer and X-Restormer perform much worse over the other comparison networks on this task. After inspecting the results, we find that these two models do not process some haze images. This suggests that these two networks may have fatal optimization difficulty in handling multi-task image restoration when dehazing is considered. Nevertheless, we can see that the introduction of task prompts effectively mitigates this problem, as depicted in Table 1 of the main paper.

## B EXPLORATION ON DIFFERENT PROMPT INTERACTION MECHANISMS

In this section, we explore the impact of different prompt interaction mechanisms in the proposed VPIP framework. A model without using prompt and two models using common modulation strategies (i.e., global feature modulation (GFM) [19] and spatial feature transform (SFT) [42]) for low-level vision tasks are compared. All models are trained on the same settings involving 30 tasks. In Table 7, we present the quantitative results of these models on restoration tasks. We can see that the model without using prompt performs much worse than other models. This is reasonable because the model

cannot handle tasks with different target domains (e.g., edge detection), which greatly affects the optimization. Models with GFM and SFT can achieve much better performance than the model without prompt interaction, but their performance is still lower than our model. This suggests that the feature modulation schemes can also achieve task guidance to a certain extent, but their ability to learn the task representation is not as effective as prompt cross-attention.

## C COMPREHENSIVE COMPARISON BETWEEN PROMPTGIP AND OUR GENLV

We conduct comprehensive experiments and demonstrate the quantitative comparison of PromptGIP and GenLV under three training settings. Trained only for restoration tasks, we can see that our GenLV\* can already outperform PromptGIP\*. This is mainly due to the powerful backbone that our VPIP framework can use. When the number of tasks increases to 15 (i.e., the PromptGIP setting), the performance of both PromptGIP# and GenLV# decreases slightly, while no more than 0.5dB. As the complexity of tasks continues to increase (i.e., the GenLV setting), we can find that the performance of both PromptGIP† and GenLV† drops significantly. However, the performance degradation of GenLV† on most tasks is within 1dB, while PromptGIP†’s performance degradation is around 2 to 4dB. This intuitively indicates that PromptGIP is more easily affected by the increase in the number and complexity of tasks. From the main paper, we illustrate that this is because PromptGIP is sensitive to the prompt content. When more tasks involving low-frequency processing are considered, its performance would be greatly affected. Many cases in the visual comparison (in the main paper Figure 5, Supp. Figure 1, 2 and 3) can more directly reflect this point.

## D COMPUTATION COST BREAKDOWN

In Table 5, we present the computation cost of different components of our GenLV model. The computational cost of the main network is similar to the original X-Restormer. The computational cost of prompt encoder comes from the residual blocks. The computational cost of the extra fusion part is from the prompt cross-attention modules in PCABs. Our prompt interaction scheme can bring considerable performance improvement at limited additional cost.

**Table 5: Computation cost of different parts of our model.**

Component	Params	MACs
Main Network	27.6M	166.9G
Prompt Encoder & Fusion	5.1M	35.7G

## E MORE VISUAL RESULTS

In Figure 5 of the main paper, we show the visual results of 9 representative tasks across different methods. In Figure 8, Figure 9 and Figure 10, we present more visual results on the remaining 21 tasks. We can see that GenLV produces the best visual results in various low-level vision tasks, with the sharpest textures and no blocking artifacts and color distortions.

**Table 6: Quantitative results (PSNR) of different image restoration backbone networks.**

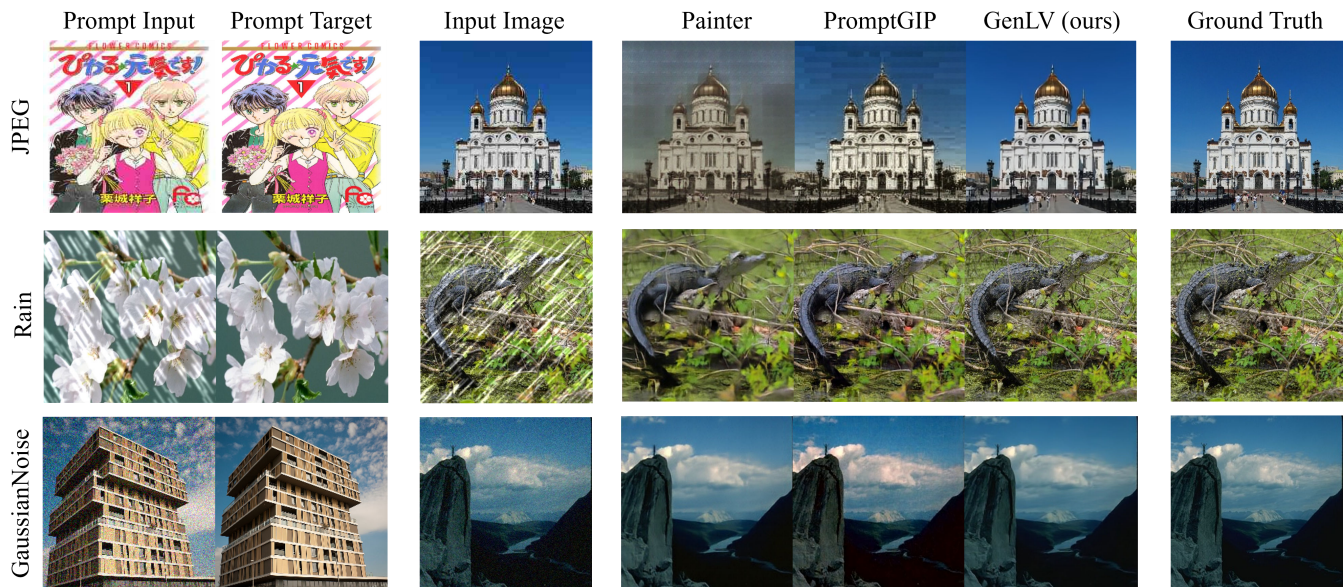
	GN	PN	S&P Noise	GB	JPEG	Ringing	R-L	Inpainting	SimpleRain	ComplexRain	Haze
RRDB	26.05	27.42	24.85	22.77	25.37	24.51	25.01	24.28	24.20	22.69	21.54
ViT	24.67	25.39	23.71	22.17	24.76	23.89	24.09	23.11	23.21	23.04	24.91
SwinIR	28.83	31.19	36.59	23.45	26.65	26.00	29.51	27.00	29.78	22.26	21.23
Restormer	28.56	31.21	35.42	24.16	26.65	27.00	29.83	27.77	29.38	24.16	14.83
X-Restormer	28.70	31.36	35.33	24.13	26.68	26.88	30.01	27.68	29.65	24.39	16.73

**Table 7: Quantitative results of using different prompt interaction mechanisms.**

	GN	PN	S&P Noise	GB	JPEG	Ringing	R-L	Inpainting	SimpleRain	ComplexRain	Haze
Without Prompt Interaction	24.30	25.85	26.54	20.63	19.26	16.88	17.87	22.57	19.56	21.55	14.22
Feature Modulation - GFM	27.76	30.04	32.42	22.52	25.68	24.55	25.65	26.12	25.66	24.56	28.55
Feature Modulation - SFT	28.03	30.58	33.20	22.82	26.04	24.72	26.46	26.42	26.48	24.46	28.17
Prompt Cross-Attention (ours)	28.28	30.80	33.47	23.14	26.06	25.50	27.51	26.66	27.68	25.13	28.65

**Table 8: Comprehensive comparison between PromptGIP and GenLV under three different settings. \*: trained only for restoration tasks. #: trained on the PromptGIP setting (15 tasks). †: trained on the GenLV setting (30 tasks).**

	GN	PN	S&P Noise	GB	JPEG	Ringing	R-L	Inpainting	SimpleRain	ComplexRain	Haze
PromptGIP*	26.48	27.76	28.08	22.88	25.86	25.69	27.05	25.28	25.79	24.33	24.55
GenLV*(ours)	28.99	31.69	36.63	24.58	26.91	27.74	31.50	28.11	31.10	24.71	28.91
PromptGIP#	26.22	27.29	27.49	22.77	25.38	25.45	26.79	25.02	25.46	24.08	24.32
GenLV#(ours)	28.92	31.58	36.32	24.33	26.55	27.55	31.11	27.86	30.35	24.47	28.73
PromptGIP†	23.63	23.98	25.05	20.84	22.21	23.86	24.94	22.11	23.16	21.79	21.90
GenLV†(ours)	28.49	31.05	34.20	23.39	26.21	25.78	28.21	27.17	28.18	25.11	29.70

**Figure 8: More visual results of different models on various low-level vision tasks.**

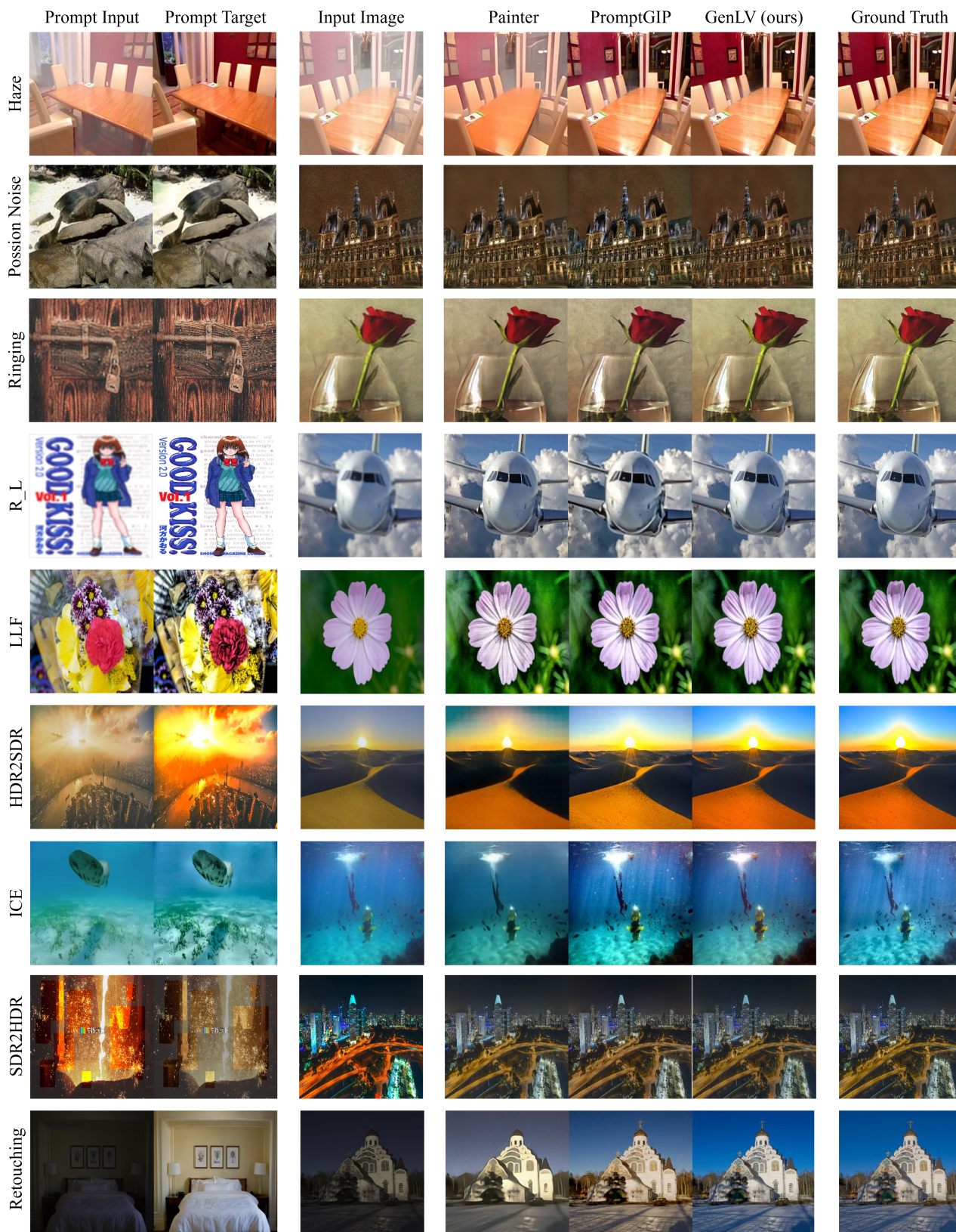


Figure 9: More visual results of different models on various low-level vision tasks.

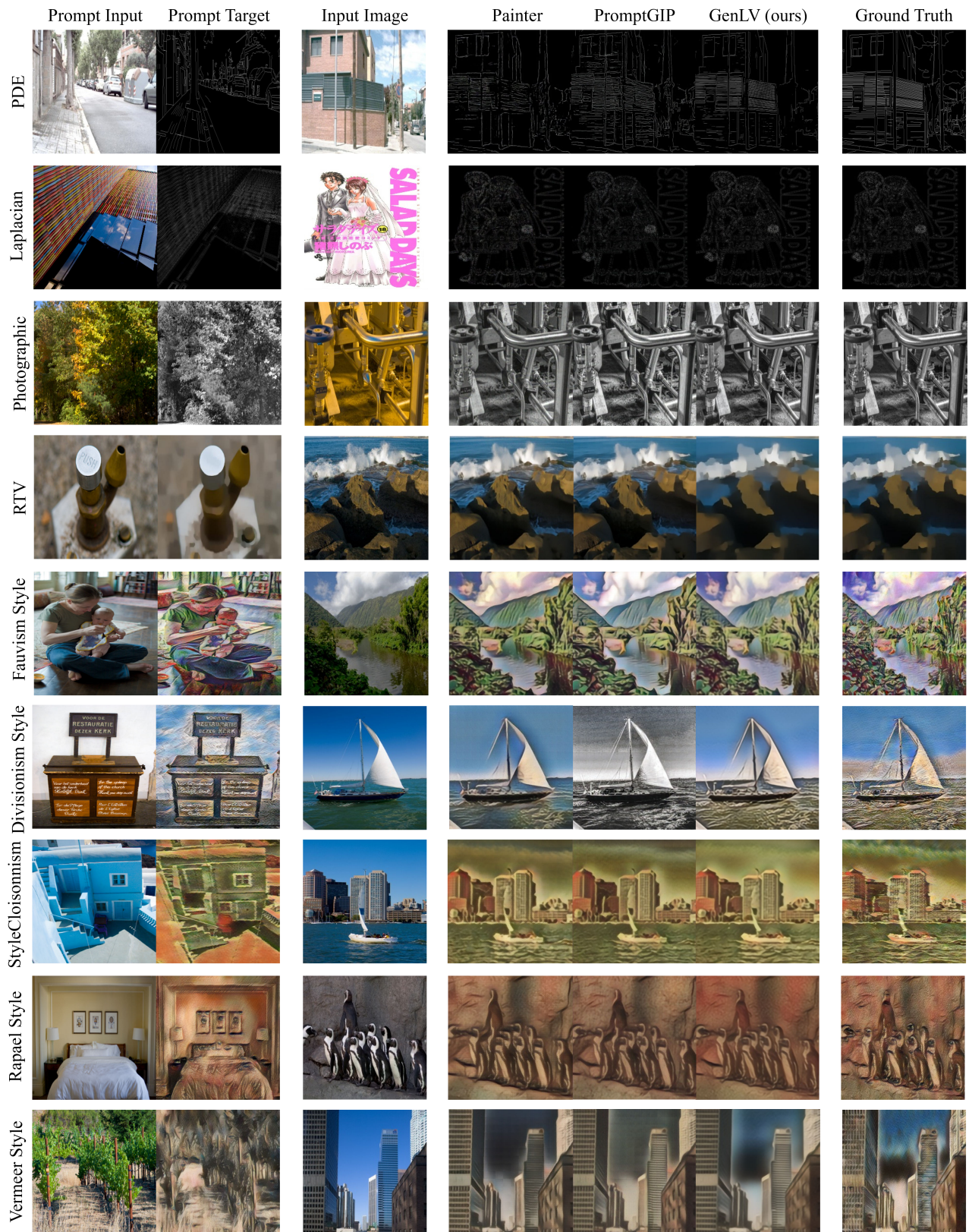


Figure 10: More visual results of different models on various low-level vision tasks.